Available online at www.sciencedirect.com

ScienceDirect

journal homepage: www.elsevier.com/locate/issn/15375110

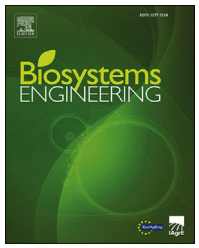

Special Issue: Biosystems and Metrology

Research Paper

An unsupervised automatic measurement of wheat spike dimensions in dense 3D point clouds for field application

Fuli Wang [a,*], *Fengping Li* [b], *Vishwanathan Mohan* [a], *Richard Dudley* [b], *Dongbing Gu* [a], *Ruth Bryant* [c]

[a] School of Computer Science and Electronic Engineering, University of Essex, Colchester, United Kingdom
[b] National Physical Laboratory, Hampton Road, Teddington, Middlesex, United Kingdom
[c] RAGT Seeds Ltd, Grange Road, Ickleton, Essex, United Kingdom

ARTICLE INFO

Article history:
Published online 11 December 2021

Keywords:
k-means
Point clouds
Shape-fitting
Unsupervised algorithm
Wheat phenotype

An accurate measurement of field-grown wheat traits, including spike number, dimension and volume are essential for crop phenotyping and yield analysis. A high-throughput method to image field-grown wheat in three dimensions is presented with an accompanying unsupervised measuring method to obtain individual wheat spike data. Images are captured using four structured light scanners on a field mobile platform, creating dimensionally accurate sub-millimetre resolution 3D point clouds for a 4.5 m^3 volume in less than 10 s. The unsupervised method analyses each trial plot's 3D point cloud, containing hundreds of wheat spikes, calculating the average size of the wheat spike and total spike volume per plot. The analysis utilises an adaptive k-means algorithm with dynamic perspectives, to fit each spike's shape and measures the dimensions with a random sample consensus algorithm. The method generates small cuboids to fit all the wheat spikes and estimate the total spikes volume. Experimental results show that the proposed algorithm is a reliable tool for identifying spikes from wheat crops and identifying individual spikes. Compared with the manual measurement, according to the results of five scenes, the average error rate in the number of spikes, spikes' height and spikes' width in tests were 16.27%, 5.24% and 12.38% respectively.

1. Introduction

Plant phenotyping is a vital tool for the development of new crop varieties and requires the undertaking of many trial growth programs, measuring and analysing trait variations over many seasons. Accurate and repeatable trait measurement is essential for success in phenotyping application. The major phenotypes for wheat breeding are the number of spikes, spike length/wide and volume. However, data collection of spike size is still primarily conducted with manual sampling (Torres & Pietragalla, 2012). A number of techniques have been explored for

* *Corresponding author.*
E-mail address: fuli.wang@essex.ac.uk (F. Wang).
https://doi.org/10.1016/j.biosystemseng.2021.11.022
1537-5110/

Nomenclature

2D	Two-dimensional
3D	Three-dimensional
RANSAC	Random sample consensus
DBSCAN	Density-based spatial clustering of applications with noise
RGB	Red Green Blue
CAD	Computer-aided design
Alg. 1	Algorithm 1: Obtaining wheat spikes
Alg. 2	Algorithm 2: Adaptive k-means algorithm based on dynamic perspectives
$Error_1$	Error rate in the number of spikes
$Error_2$	Error rate in the spike height
$Error_3$	Error rate in the spike width

collecting data for quantitative studies of complex traits related to the growth, yield and adaptation to biotic or abiotic stress (see (Lei Li et al., 2014) and references therein). Spike counting is one of the main approaches for predicting grain yield in wheat and other cereals (Pask et al., 2012). To count the number of wheat spikes, Deery et al. (2014) used a simple particle count algorithm on segmented 2D images but was unable to address the challenge of high crop density and overlapping spikes. Reducing count errors in dense, close contact spikes was explored by Fernandez-Gallego et al. (2018), using an automatic spike-counting algorithm and zenithal colour 2D images of the crop in natural light conditions. Algorithms such as DeepCount (Sadeghi-Tehran et al., 2019; Tan et al., 2020) have been developed to count the number of wheat spikes in 2D images using the deep convolutional neural networks and machine learning approaches. Achieving volumetric or dimensional information is challenging, especially when taken from directly above or from an angle where distortions are introduced and only partial visibility mask the real size of the spike. Calibration charts can mitigate distortions and mosaicking errors, but there are complex to implement for high-throughput field studies.

Generating a 3-D, digital twin of a wheat plot offers a much richer and dimensional correct representation, overcoming issues of obscured and overlapping spikes. Generating the digital twin is achieved by combining multiple 2D images or utilising more complex imaging technology such as Lidar, time-of-flight or structured light scanners (Mohamed & Dudley, 2019). The field captured data is no longer represented by a 2D RGB image but a 3D point cloud with format P_n (x, y, z, RGB). Algorithms used for 2D image analysis are no longer applicable for point clouds and alternative approaches have been developed using supervised neural networks to fit complex geometric primitives, such as CAD models of mechanical components (Lingxiao Li et al., 2019; Su et al., 2018). However, by using a more classical clustering algorithm to segment the wheat, and then subsequently fitting to spikes, the process of training a supervised model can be omitted, and the fitting results can be obtained with less time cost. For example, Velumani et al. (2017) performed wheat spike segmentation using two different classical methods: voxel-based segmentation and mean shift segmentation. Additionally, density-based spatial clustering of applications with noise (DBSCAN) algorithm (Ester et al., 1996) has been developed for the task of segmentation, and then least−squares curve fitting is used to obtain the size of the wheat spikes (Thompson et al., 2019). Although the clustering algorithms such as DBSCAN, mean shift and k-means can be successful in segmentation tasks, the segmentation task can be challenging for these algorithms in specific complex environments, such as when wheat crops are very dense. Our recent work has proposed an adaptive k-means algorithm with dynamic perspectives, which performs segmentation to separate the wheat spikes, to tackle this challenge (Wang et al., 2020). Although this algorithm can be applied in an environment where multiple wheat spikes are grown densely, it still cannot address more than one hundred wheat spikes. As shown in Fig. 1, compared with sample wheat crops in lab, the captured 3D point cloud images from the field usually have hundreds of spikes and can contain noise, which makes it difficult for the existing measurement algorithms to obtain a robust measurement result. This paper contributes to filling this gap by providing an unsupervised framework to tackle 3D point cloud images with hundreds of wheat crops from the field.

To realise the field application, the proposed k-means algorithm needs to separate the wheat spikes, remove the stems and then obtain the spikes. Since there are hundreds of wheat spikes, the method randomly selects some areas as sample areas and calls the adaptive k-means algorithm to calculate the average spike size. Meanwhile, the algorithm segments all of the spikes as thousands of small segments and uses

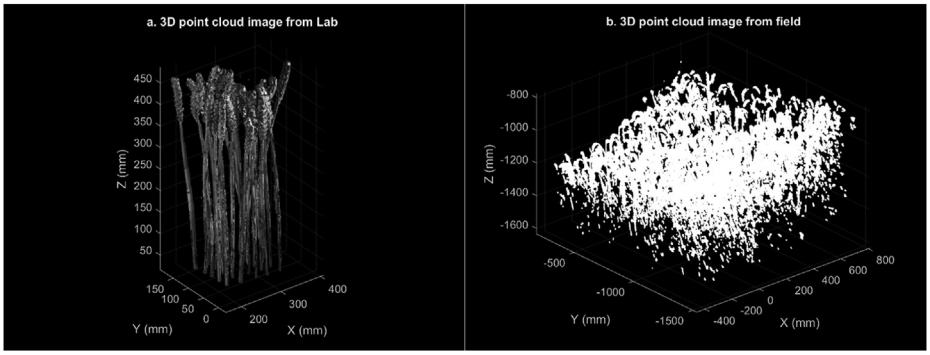

Fig. 1 – 3D point cloud images of wheat crops.

cuboids to fit each segment and estimate the total volume of all spikes. The number of wheat spikes can be approximately estimated according to the average size and total volume. The proposed method is described in detail in section 3.

2. The adaptive k-means algorithm with dynamic perspectives

2.1. Classical clustering algorithms

The clustering algorithms are useful tools for the task of separating spikes from wheat crops in the point cloud. As discussed in the introduction, there are not many complex geometric primitives in wheat crops. The DBSCAN and k-means algorithms are well suited to the task, but some defects still exist when dealing with some practical situations. One of the disadvantages of the DBSCAN is that the performance depends largely on the selection of parameters, but there is no theoretical guidance for setting its parameters. Therefore, the trial method is used commonly, but it relies on experience, which results in the final parameters not necessarily being optimal (Lai et al., 2019). However, k-means has the characteristics of a single parameter, and its parameter k represents the cluster number. To compare these two classical algorithms, Fig. 2 demonstrates the segmentation results of the DBSCAN (*the minimum number of neighbours is set as 10, the neighbourhood radius is set as* 5) and classical k-means ($k = 12$). As there are 12 spikes, we set the parameter of k-means as 12 and used the trial method to set the relatively reasonable parameters of the DBSCAN. The DBSCAN algorithm can only roughly divide the 12 spikes into four segments; in other words, DBSCAN identifies that there are only four spikes (with different colours in Fig. 2a), which is quite different from the actual situation. Meanwhile, in the classical k-means algorithm, even if we set the number of clusters to 12, the output result is still not satisfactory. These narrow results illustrate that the classical clustering algorithm cannot handle some complex environments such as when wheat crops are very dense.

2.2. The k-means algorithm based on dynamic perspectives

To address the above concerns, the adaptive k-means algorithm with dynamic perspectives was used. To demonstrate this idea, as is shown in Fig. 3, when wheat crops are observed from the side, which part is the wheat spike and which part is the stem can be easily distinguished. Due to overlapping between the spikes, how many spikes cannot be easily judged from the side view (Fig. 3a). However, the top view can be used to count the number of spikes (Fig. 3b). Similarly, for the k-means algorithm, if all of the 3D points are projected into the 2D top view, the point distance in the within-cluster is reduced and clustering performance will be improved.

To improve segmentation performance, the above idea was introduced into the k-means algorithm. The flowchart of the k-means algorithm with dynamic perspectives can be seen in Fig. 4. Specifically, given a cluster consisting of points $N_{n\times3}$ (Fig. 4a), where n is the number of points, and 3 is the number of dimensions, we denote by $\{x_i\}$, $\{y_i\}$ and $\{z_i\}$ the x, y and z coordinates of the point $i(i \in n)$. For the side view, we transfer the $N_{n\times3}$ array into an $N_{n\times2}$ array, which only contains the two dimensions of $\{x_i\}$ and $\{z_i\}$. The 2D points were inputted from the side view into the k-means, which outputs all point labels. Using the labels to mark all 3D points, the clustering result in Fig. 4b were achieved. To separate spikes

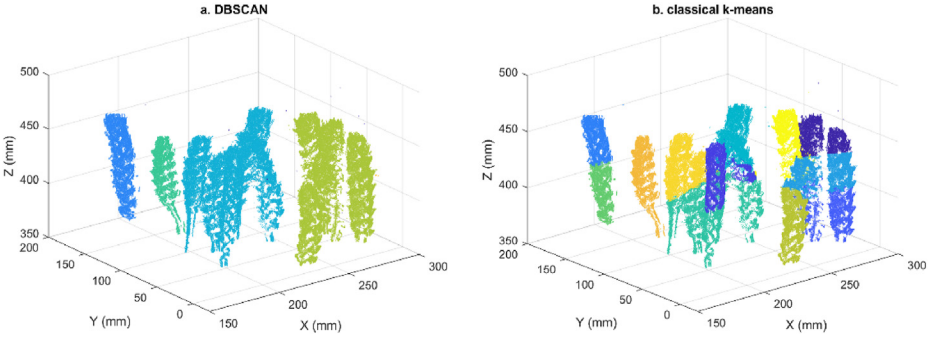

Fig. 2 – Results of DBSCAN and classical k-means segmentation.

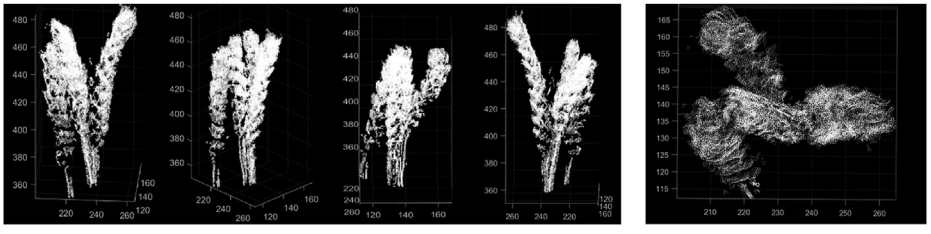

a) Side views b) Top view

Fig. 3 – The spikes observation with dynamic perspectives.

from the wheat (Fig. 4c), Algorithm 1 (Alg. 1) is defined to preserve the top segments. Similarly, transferring the 3D points of spikes into the top view $N'_{n\times2}$, which only contains two dimensions of $\{x_i\}$ and $\{y_i\}$, we obtain the segmentation result based on the top view in Fig. 4d, which is better than the classical algorithms results. Finally, a random sample consensus (RANSAC) algorithm (Schnabel et al., 2007) was used to fit each segment shape and obtain the dimensions as shown in Fig. 4e.

In Alg. 1 defined below, a value space according to the highest point of all 3D points was defined which has the max value of $\{Z\}$. By extracting all the segments in the value space, the points belonging to spikes are obtained. As is shown in Fig. 5, the highlighted area is the value space which is determined by the parameter σ. Once this value space was defined, to preserve the top segments, only whether the highest point of each segment is located in this space was required. By using this operation to preserve the top segments, the space value does not have to be set too accurately; it is sufficient to ensure that σ is a small value (Fig. 5a,b are both the correct spaces that can output the same result). Note that, if we change the conditional statement in Alg.1 to judge whether the lowest point of each segment is located in this space, the σ would be set to a larger value (in the case of Fig. 5c). In this paper, the former conditional statement (with σ set to 60 mm) was used and use statistical filtering reduced the noise.

As can be seen from Fig. 4, it is sufficient to set the k-means parameter to 3 or 4 for the side view. Since the shape of the wheat crop is similar to a cuboid or cylinder, selecting the side view from the X or Y direction will obtain the same final result. Further, shape fitting for each spike is required with the number of clusters set in advance, that is, the number of spikes. In Fig. 4, k was set to 12 for the top view. However, in practical application, it is impossible to know how many wheat spikes there are in advance. This means that it was expected that the algorithm can calculate the number of spikes by itself. To realise this function, this paper adds an adaptive operation to self-update the appropriate parameter values. The detail of this adaptive k-means algorithm based on dynamic perspectives is described in Alg. 2.

In the algorithm, an initial parameter k' is required to perform the segmentation for the top view. The value of this initial parameter should be a small number as the algorithm can update it adaptively. In this paper, to set the initial value, DBSCAN provided by Rolf Harkes (2018) was used which makes use of the k-d trees spatial partitioning algorithm, because the DBSCAN can roughly divide the spikes into a few segments, which is far smaller than the actual number of spikes. After obtaining the initial parameter k', the algorithm uses k-means to segment the 2D points of the top view and then calls the RANSAC algorithm to fit a cuboid to each segmentation. Since the initial value of k' is small, the fitting

Algorithm 1: Obtaining wheat spikes

Require: 3D points: $N_{n\times3}$;

Initialize parameter of σ;

Reduce the noises of 3D points;

Obtain side view 2D points: $N_{n\times3} \rightarrow N_{n\times2}$

Use the k-means for segmentation based on side view;

Obtain the point with the highest Z coordinate value: $Z_{\max}$;

Calculating a value space of Z coordinates:

$$[Z_{\max} - \sigma, Z_{\max}]$$

For each highest point within its segment:

    If the highest point is located in the value space: Preserve this segment

    else: continue;

return all preserved segments.

result is not accurate. As is shown in Fig. 6a, when the k' is small, some abnormal spike sizes will be outputted (the fitting size of the purple part is significantly larger than that of regular wheat). Therefore, once the algorithm detects unreasonable results, the k' will be superimposed until a reasonable final result is outputted (Fig. 6b). The last updated k' value is the number of spikes counted by the algorithm.

algorithms, it is still challenging to directly apply Alg.2 with images captured over a wide area such as shown in Fig. 1b. Suppose we directly use Alg.2 to deal with these images, as there are so many noises and wheat crops, the computational efficiency will be significantly reduced. Besides, due to noise interference, it is difficult to output an ideal result without abnormal size.

Algorithm 2: Adaptive k-means algorithm based on dynamic perspectives

Obtain the wheat spikes according to Alg.1

Set the initial parameter k' for the top view

Obtain top view 2D points: $N'_{n\times 3} \rightarrow N'_{n\times 2}$

repeat

Use the k-means for segmentation based on top view;

Use RANSAC to fit each segment;

Evaluate the size of each segment;

if (there is an abnormal size)

k'++;

break;

end if

until there is no abnormal size

return the updated shape model.

Note that the algorithm did not make any intrinsic change to the k-means algorithm, and instead, it required several iterations of any existing implementation of k-means. Therefore, the algorithm can call any version of the k-means algorithm. Considering the computational performance, it is recommended to use Lite k-means (Cai, 2011) or ball k-means (Xia et al., 2020) to run the proposed algorithm.

3. The framework of the proposed method for wheat field application

Although Alg. 2 can deal with the environment where multiple wheat spikes are grown densely better than classical

To address the above problem, as is shown in Fig. 7, our proposed method was extended based on Alg. 2. Firstly, the original field image was divided into a few segments, and some stems are removed. As can be seen in Fig. 7, the original image was divided into three segments, then the spikes volume of each segment was calculated separately. To calculate the volume, 3000 small cuboids were used to fit the shape of all spikes for each segment. There is an illustration to show the volume calculation method in Fig. 8; in this example, there are 50 cuboids to realise the shape fitting of 3 spikes, so the volume of spikes is the sum of the volumes of all cuboids. After the volume calculation, some small areas were selected as sample areas (the red highlighted areas in Fig. 7), then Alg. 2 was used to calculate the average size of these areas. Overall,

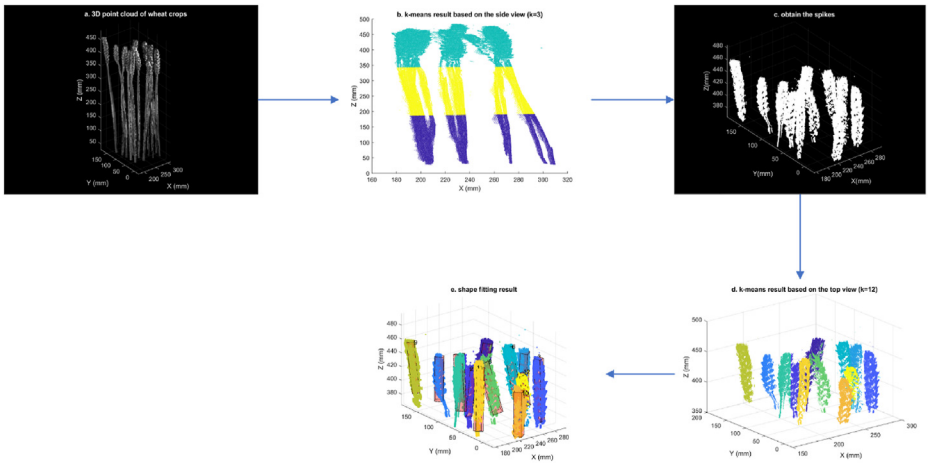

Fig. 4 – Segmentation results base on the proposed *k*-means.

for images from the wheat field, the total spikes volume and the average size of a single spike could be estimated by the proposed method.

The above description involves two parameters. The first is the number of segments and the second is the number of small cuboids. In this paper, all of the original images were divided into 3 segments and 3000 cuboids used to deal with each segment. If the value of these parameters increases, the accuracy of the calculation results might be improved, but it would also increase the calculation cost.

4. 3D field capture

Imaging technologies applicable for field capture include time-of-flight cameras, structured light scanners, and stereo RGB. To understand the performance of each system a series of commissioning tests were undertaken (Mohamed & Dudley, 2019). Our aim was to construct a portable, field-deployable solution that could completely image a field-grown trial plot, dimension 2 × 5 × 1 m, in less than 1 s

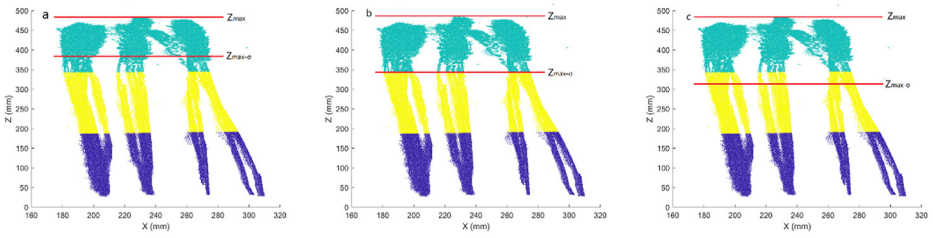

Fig. 5 – Three different value spaces for spikes obtaining. From *a* to *c*, the value σ gradually increases.

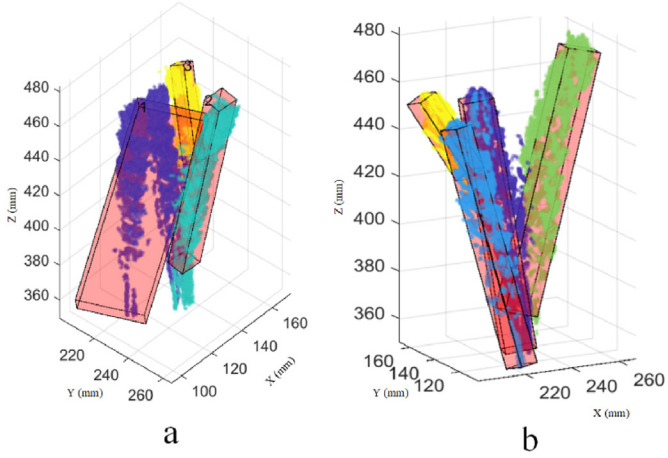

Fig. 6 – (a) The shape fitting result with abnormal sizes ($k' = 3$); (b) the final shape fitting result ($k' = 4$).

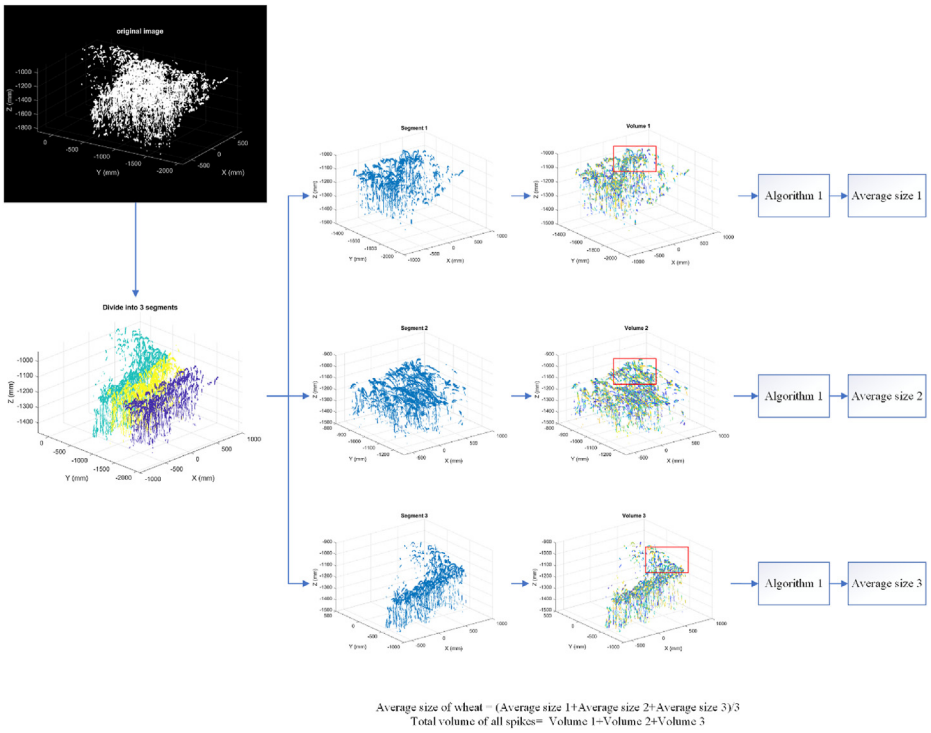

Fig. 7 – Overall flowchart of the proposed method.

ready for analysis with wheat identification algorithms. The platform had to be easily moved between plots, deal with typical weather conditions including direct solar illumination and be self-powered. The solution deployed in the fields during 2020 is shown in Fig. 9, which included four structured light scanners from Photoneo (Photoneo s.r.o., Bratislava, Slovakia) each positioned parallel to one side of the trial plot edge and orientated at 45° to the vertical. The arrangement ensured the capture of the central region of the plot only neglecting 300 mm around the edges which are normally excluded from analysis in most trials. Each scanner was triggered in sequence to avoid interference and a region of $2 \times 2 \times 1.5$ m was captured in approximately 5 s. The scanners were optimised to overcome bright ambient light using structural netting above and to the sides of the mounting frame, but also critical was the selection of the scanner's exposure, laser brightness and processing algorithms.

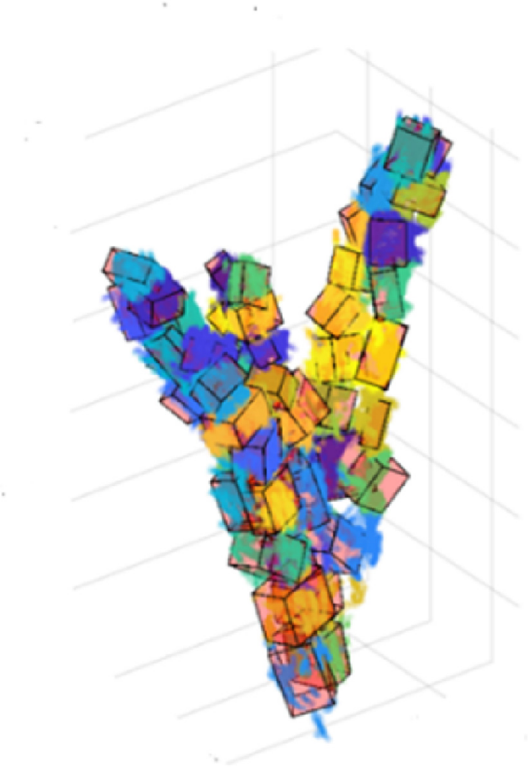

Fig. 8 – An example of volume calculation method by using cuboids fitting.

Reconstructing the four independent Photoneo scans into a single point cloud was achieved using a common reference chart placed in view of all scanners, this is just visible in Fig. 9. Unlike single point measurement systems, our final point clouds include information of the complete surface for all the wheat heads with detail down to grain level. The final point clouds were cleaned for noise using a statistical outlier filter and the resolution was reduced with a sub-sampling algorithm to reduce the computational power needed for the next stage of processing, identifying spikes and performing dimensional measurements.

In total 25 trial plots were captured over 3 h with delays primarily caused by physical movement of the platform around rows, failed captures from wind motion and some data management tasks not yet fully automated. However, with further optimisations, it was estimated that a single platform of this type would be able to capture between 100 and 250 trial plots per working day.

Fig. 9 – Field use of 3D capture system incorporating 4 Photoneo L scanners.

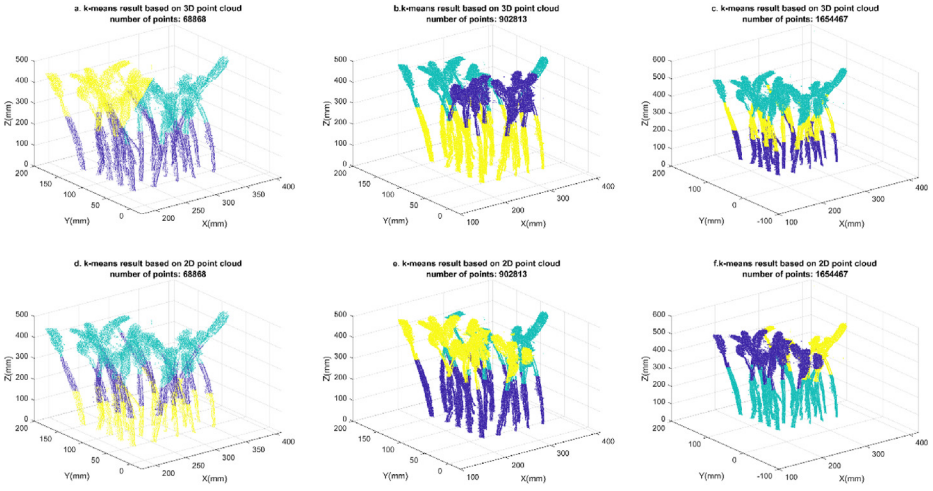

Fig. 10 – Results of *k*-means based on 3D and 2D point clouds.

5. Experimental results and discussion

In this section, a series of 3D point cloud images captured from the laboratory was used to test the performance of the proposed *k*-means algorithm. Five different field plots that were captured by our platform were selected and cropped to test the whole proposed measurement method.

5.1. *The analysis of the proposed k-means algorithm*

The proposed *k*-means algorithm is a two-stage method. In the first phase (Alg.1), the projection of a 3D point cloud image into a 2D point cloud (side view) is a dimension reduction process. In order to test that this dimension reduction can not only output good results but also improve the speed of the algorithm, some experiments were carried out and the results shown in Fig. 10.

As shown in Fig. 10, for the same scene of the 3D point cloud, the number of points was adjusted by down sampling. The algorithm was run five times to calculate the average results that were implemented in MATLAB R2020b based on a Core i9-9980HK CPU 2.40 GHz laptop. The comparison running time between 3D and 2D point clouds is shown in Table 1. It indicates that using *k*-means to process 3D and 2D point cloud images, the results were similar, but with the increase of points, the computational efficiency of the 2D point cloud was improved. Note that the running time included the whole time from loading the point cloud to drawing the resulting picture. Additional, the Lite *k*-means was used to obtain these results,

Table 1 – The comparison running time between 3D and 2D point clouds.

Number of points	Running time of 3D point cloud	Running time of 2D point cloud
68,868	1.91 s	1.67 s
902,813	9.28 s	8.69 s
1,654,467	16.86 s	15.12 s

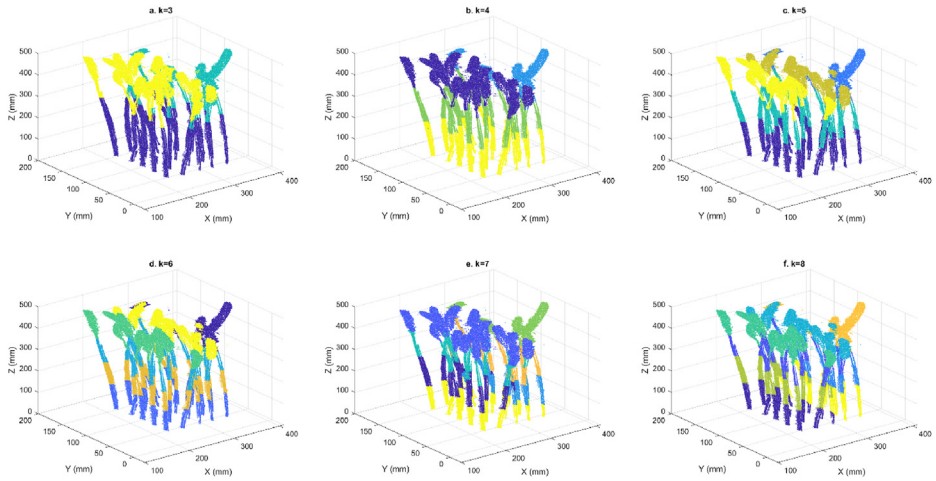

Fig. 11 – The clustering results with different values of *k*.

compared with the traditional *k*-measure, Lite *k*-means process significantly improved the calculation speed by using the operation mechanism of MATLAB.

Further, in the first phase, the parameter (*k*) of *k*-means was not expected to have a great impact on our expected result. To verify this, Fig. 11 shows the clustering results with different values of *k*.

Since the proposed algorithm only needs to preserve the top segments to obtain the spikes, all of the results of Fig. 11 can be used, but if a small *k* value is selected, a portion of stems will be considered as part of the top segments. This will introduce an error in spike height. If a bigger value of *k* is chosen, the stem points counted might be less. However, it cannot be guaranteed that there is a perfect parameter value to completely remove all of the stem's points. Also, as the value of *k* increases, the efficiency of the algorithm might be reduced. This will be discussed in the next section.

For the second phase (Alg.2), the projection of the 3D point cloud image onto the 2D point cloud (top view) is more important. This is because the height of the spike is longer than the width and length in 3D space, projecting the 3D image onto a 2D top view can reduce the point distance in within-cluster, which can improve the algorithm to identify the individual spikes. To validate the performance of this phase, different scenes were tested with the proposed algorithm. As shown in Fig. 12, in these three scenes, some of the wheat crops were dense or mutually overlapping (highlight areas), but from the clustering results, the proposed method

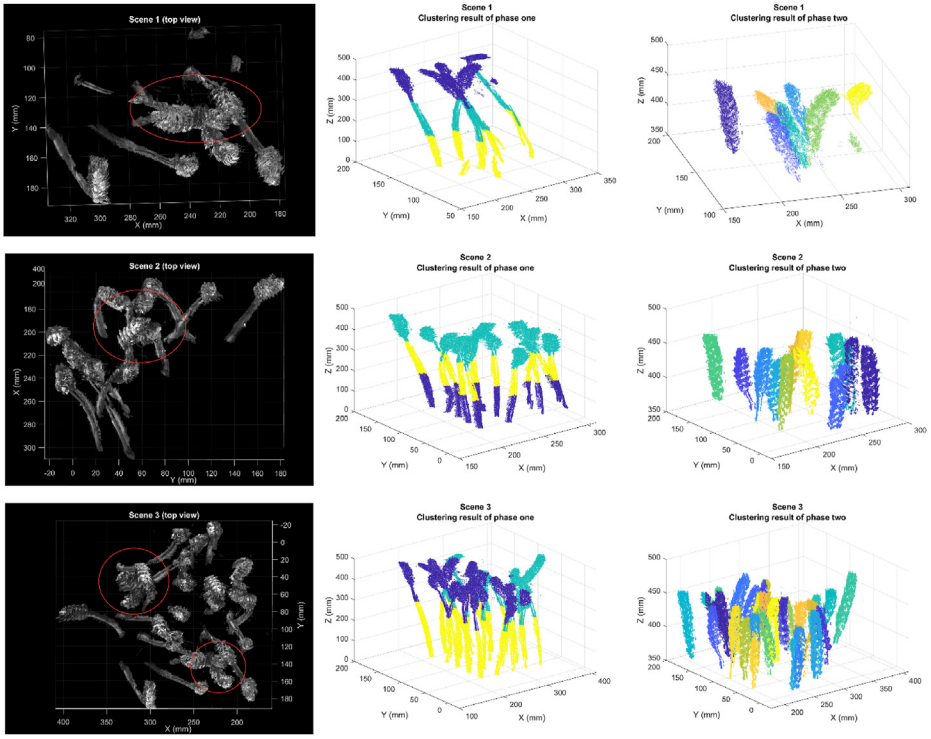

Fig. 12 – Clustering results with different scenes.

Table 2 – The average running time of the proposed algorithm.

Scene number	Number of points	Running time for phase one	Running time for phase two
1	166,283	3.26 s	44.27 s
2	747,982	8.84 s	184.13 s
3	902,813	12.51 s	377.68 s

still shows some robustness and feasibility, especially compared with the traditional algorithm results in section 2.1.

5.2. *The efficiency analysis of the proposed algorithm*

To analyse the efficiency of the algorithm, the same laptop mentioned above ran the algorithms for different situations of the wheat crops. For the three situations in Fig. 12, the algorithm was run 5 times for each situation and the average time recorded. The value of k was set as 6 for phase one (Alg. 1) and max iterations of the RANSAC algorithm (in phase two) as 1000. The average running time of phase one and phase two is recorded separately in Table 2.

As can be seen from Table 2, thanks to the performance of Lite k-means, the k-means in the proposed algorithm did not consume many computing resources. Comparing Table 1 with Table 2, the different parameter values that can influence the calculation time can be seen but the changes are not large (in Table 1, k is 3). However, in phase two, the algorithm operates with self-adaptive updating of the parameters and calls the RANSAC to fit the shape of each cuboid, and this part plays a key role in the efficiency of the algorithm. Throughout the whole process, the efficiency of the algorithm in processing wheat was good. Furthermore, the running time for handling a field image was tested. The testing image is shown in Fig. 13. For the volume calculation, the main calculation time was to divide all spikes into 3000 segments, and the RANSAC called to fit each segment to evaluate the total volume. Therefore, the parameter k was set as 3000 to carry out the segmentation and then realise shape fitting. The whole running time was 36.7 min.

According to the above experiments, it can be seen that the proposed method consumes most computing time when calculating the total volume of spikes. This is because the method needs to call the RANSAC 3000 times to fit the shape of each small segment. Overall, the proposed algorithm can evaluate the sampled spike size with high efficiency. For the volume calculation of spikes, using the proposed method, it takes about 30–40 min to complete the volume calculation once on a standard modern laptop.

5.3. *Comparison of manual measurement with the proposed method*

The method proposed in this paper can be applied to the scenario of hundreds of wheat crops. Therefore, this section describes experiments to validate the proposed method compared with manual measurement. Five different scenarios were tested with this method, each scenario is around one square metre of a wheat field, and the original images used are shown in Fig. 14.

For manual measurement, a sample area is usually selected in the field. The number and size of spikes in the sample area are measured to infer the total number and average size of wheat crops in the entire field. In this experiment, for each scenario, we selected a 0.25 m^2 square as the sample area. The number of spikes n_m were counted and the average size of spikes (height h_m and width w_m) in the sample area was measured. The amount of wheat (spikes m^{-2}) was calculated according to the following equation:

$$num_m = \frac{n_m}{0.25} \tag{1}$$

The proposed method calculated all spike total volume V_a and the average size of the single spike. Note that Alg. 2 can output the height, length and width (h_a, l_a, w_a) of the spike and cuboid fitting was used to facilitate comparison with manual measurement. The values h_a and $w'_a = (l_a + w_a)/2$ were used to compare with h_m and w_m. As each tested scenario is about one square meter of a wheat field, for the proposed method, spikes total volume was divided by the single spike volume to

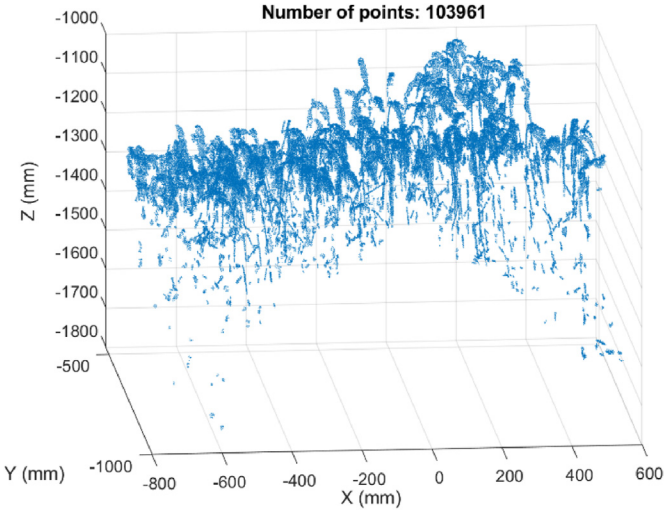

Fig. 13 – Example of a segment of field image for the run-time test.

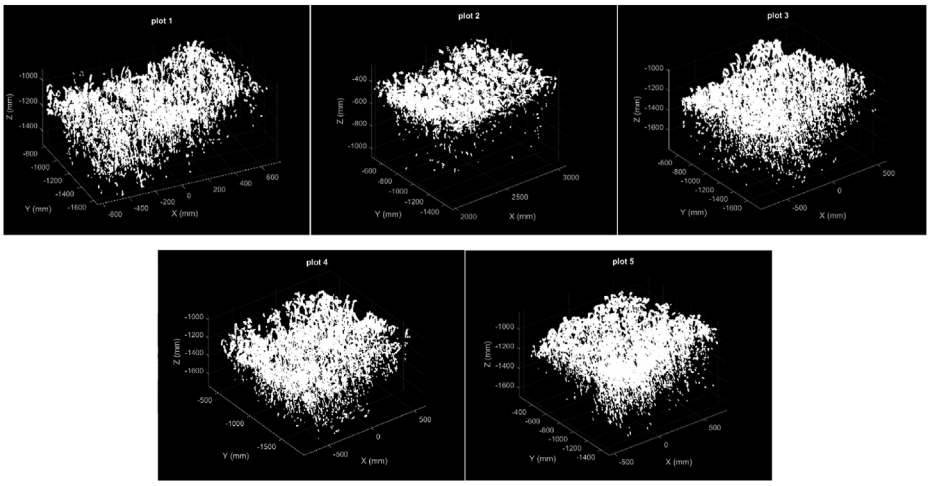

Fig. 14 – Five different 3D point images from the field.

estimate the number of spikes in each scenario according to the following equation:

$$num_a = \frac{V_a}{h_a \times w'_a \times w'_a} \quad (2)$$

The comparison results are recorded in Table 3. To compare the proposed method with the manual method, the following equations were used to estimate the error rate of each plot:

$$\text{Error rate in the number of spikes: } Error_1 = \frac{|num_m - num_a|}{num_m} \quad (3)$$

$$\textit{Error rate in the spike height } Error_2 = \frac{|h_m - h_a|}{h_m} \quad (4)$$

$$\textit{Error rate in the spike width} : Error_3 = \frac{|w_m - w_a|}{w_m} \quad (5)$$

As we can see in Table 4, in the five experiments, the three average error rates defined above were 16.27%, 5.24% and 12.38% respectively.

5.4. *Discussion*

From all of our experiments, we made a detailed analysis of the proposed *k*-means algorithm. Although *k*-means is an uncertain algorithm that cannot guarantee that the output is always the same, for our proposed algorithm the clustering result was good enough for shape fitting. Additionally, the shape fitting algorithm is not the focus of this paper although it was discovered by using the cuboid fitting that the fitting result for straight spikes was better than for the curved ones. This is because cuboids cannot accurately fit the height of curved wheat spikes. Furthermore, as shown in Table 3, all of the average heights obtained by the proposed algorithm were slightly smaller than that measured manually. This was because most of the tested wheat spikes were slightly curved, and there would be some errors when using cuboid shape fitting. Besides the shape fitting algorithm, with the spikes being more curved, the overlapping in the plan view will be obvious. This might influence the clustering result of the proposed *k*-means algorithm.

Further, there are still a few issues in our method which might be considered to address in future work. First, a self-adaptive *k*-means algorithm to update the *k* iteratively in Alg.2 was proposed for spikes counting. However, for volume calculation, the computational efficiency was not very good. Therefore, when we dealt with the field images, we divide the whole image into three segments. Secondly, as mentioned above, the accuracy of this method was affected by the curvature of the spike. Five field data set results were used and the average error in the number of spikes was greater than 16%, of which two errors were greater than 20%. The performance of the algorithm might decrease if this analysis was extended to spike dimensions assessment for other field data sets.

Table 3 – Comparison results between manual measurement and the proposed method.

Plot number	Average size		Number of spikes		Total volume
	Manual h_m/w_m	Proposed method h_a/w'_a	Manual num_m	Proposed method num_a	V_a
1	83.4/13.5 mm	76.7/12.4 mm	212	173	2,042,491 mm^3
2	71.9/15.5 mm	63.6/14.6 mm	260	202	2,766,830 mm^3
3	84.2/14.2 mm	81.8/18.2 mm	200	259	7,020,030 mm^3
4	82.4/15.2 mm	81.3/17.6 mm	212	207	5,179,640 mm^3
5	78.3/15.0 mm	76.4/15.6 mm	228	208	3,866,860 mm^3
Standard Deviation	5.1/0.8 mm	7.4/2.3 mm	/	/	/

Table 4 – Error rates of the proposed method.

Plot Number	$Error_1$	$Error_2$	$Error_3$
1	18.40%	8.03%	8.15%
2	22.31%	11.54%	5.81%
3	29.5%	2.85%	28.17%
4	2.36%	1.34%	15.79%
5	8.77%	2.43%	4%
Average	16.27%	5.24%	12.38%

Overall, all of the experiment results imply that our method has a good potential to be developed as a tool to evaluate the size and yield of wheat spikes, especially for straight spikes, whilst avoiding the time-consuming and tedious manual measurements.

6. Conclusion

A high-throughput field capture platform for wheat combined with an unsupervised automatic measurement of wheat spikes based on an adaptive *k*-means algorithm with dynamic perspectives is proposed, which can deal with the complex environment where hundreds of wheat spikes are grown densely. This method has provided a novel framework to obtain wheat spike dimensions and total volume in the place of manual measurement. The results demonstrate a level of robustness of our method to measure the wheat spike dimensions and volume in the wheat field scenario. As method performance can still be improved to handle curved wheat spikes, our future work will further optimise our algorithm to deal with the environment where the wheat spike is arched.

Declaration of competing interest

The authors declare that they have no known competing financial interests or personal relationships that could have appeared to influence the work reported in this paper.

Acknowledgments

This work is supported by the UK Government's Department of Business, Energy and Industrial Strategy (BEIS) as part of the National Measurement System (NMS) program.

REFERENCES

Cai, D. (2011). Litekmeans: The fastest matlab implementation of kmeans. Software available at. Http://Www. Zjucadcg. Cn/Dengcai/Data/Clustering. Html http://www.cad.zju.edu.cn/home/dengcai/Data/code/litekmeans.m.

Deery, D., Jimenez-Berni, J., Jones, H., Sirault, X., & Furbank, R. (2014). Proximal remote sensing buggies and potential applications for field-based phenotyping. *Agronomy*, 4(3). https://doi.org/10.3390/agronomy4030349

Ester, M., Kriegel, H.-P., Sander, J., & Xu, X. (1996). A density-based algorithm for discovering clusters in large spatial databases with noise. *Proceedings of the 2nd International Conference on Knowledge Discovery and Data Mining*, 96(34), 226–231.

Fernandez-Gallego, J. A., Kefauver, S. C., Gutiérrez, N. A., Nieto-Taladriz, M. T., & Araus, J. L. (2018). Wheat ear counting in-field conditions: High throughput and low-cost approach using RGB images. *Plant Methods*, 14, Article 22. https://doi.org/10.1186/s13007-018-0289-4

Harkes, Rolf (2018). GitHub - rharkes/DBSCAN-for-Matlab: Using kd-trees. https://github.com/rharkes/DBSCAN-for-Matlab.

Lai, W., Zhou, M., Hu, F., Bian, K., & Song, Q. (2019). A new DBSCAN parameters determination method based on improved MVO. *IEEE Access*, 7, 104085–104095. https://doi.org/10.1109/ACCESS.2019.2931334

Li, Lei, Zhang, Q., & Huang, D. (2014). A review of imaging techniques for plant phenotyping. *Sensors (Switzerland)*, 14(11), 20078–20111. https://doi.org/10.3390/s141120078

Li, Lingxiao, Sung, M., Dubrovina, A., Yi, L., & Guibas, L. J. (2019). Supervised fitting of geometric primitives to 3D point clouds. In *Proceedings - IEEE Computer Society Conference on Computer Vision and Pattern Recognition* (pp. 2652–2660).

Mohamed, I., & Dudley, R. (2019). Comparison of 3D imaging technologies for wheat phenotyping. *IOP Conference Series: Earth and Environmental Science*, 275. https://doi.org/10.1088/1755-1315/275/1/012002

Pask, A., Pietragalla, J., & Mullan, D. (2012). Physiological breeding II: A field guide to wheat phenotyping. *Chemistry*.

Sadeghi-Tehran, P., Virlet, N., Ampe, E. M., Reyns, P., & Hawkesford, M. J. (2019). DeepCount: In-Field automatic quantification of wheat spikes using simple linear iterative clustering and deep convolutional neural networks. *Frontiers of Plant Science*, 10. https://doi.org/10.3389/fpls.2019.01176

Schnabel, R., Wahl, R., & Klein, R. (2007). Efficient RANSAC for point-cloud shape detection. *Computer Graphics Forum*. https://doi.org/10.1111/j.1467-8659.2007.01016.x

Su, H., Jampani, V., Sun, D., Maji, S., Kalogerakis, E., Yang, M. H., & Kautz, J. (2018). SPLATNet: Sparse lattice networks for point cloud processing. *Proceedings - IEEE Computer Society Conference on Computer Vision and Pattern Recognition*, 2530–2539. https://doi.org/10.1109/CVPR.2018.00268

Tan, C., Zhang, P., Zhang, Y., Zhou, X., Wang, Z., Du, Y., Mao, W., Li, W., Wang, D., & Guo, W. (2020). Rapid recognition of field-grown wheat spikes based on a superpixel segmentation algorithm using digital images. *Frontiers of Plant Science*, 11(259). https://doi.org/10.3389/fpls.2020.00259

Thompson, A., Livina, V., Harris, P., Mohamed, I., & Dudley, R. (2019). Model-based algorithms for phenotyping from 3D imaging of dense wheat crops
. *2019 IEEE International Workshop on Metrology for Agriculture and Forestry, MetroAgriFor 2019-Proceedings*, 95–99. https://doi.org/10.1109/MetroAgriFor.2019.8909214

Torres, A., & Pietragalla, J. (2012). Crop morphological traits. *Physiological Breeding II: A Field Guide to Wheat Phenotyping*.

Velumani, K., Oude Elberink, S., Yang, M. Y., & Baret, F. (2017). Wheat ear detection in plots by segmenting mobile laser scanner data. *ISPRS Annals of the Photogrammetry, Remote Sensing and Spatial Information Sciences*. https://doi.org/10.5194/isprs-annals-IV-2-W4-149-2017

Wang, F., Mohan, V., Thompson, A., & Dudley, R. (2020). Dimension fitting of wheat spikes in dense 3D point clouds based on the adaptive k-means algorithm with dynamic perspectives. *2020 IEEE International Workshop on Metrology for Agriculture and Forestry, MetroAgriFor 2020-Proceedings*, 144–148. https://doi.org/10.1109/MetroAgriFor50201.2020.9277611

Xia, S., Peng, D., Meng, D., Zhang, C., Wang, G., Giem, E., Wei, W., & Chen, Z. (2020). A fast adaptive k-means with No bounds. *IEEE Transactions on Pattern Analysis and Machine Intelligence*, 44(1), 87–89. https://doi.org/10.1109/tpami.2020.3008694